Wear Properties of Wood-plastic Composites Pretreated with a Stearic Acid-palmitic Acid Mixture before Exposure to Degradative Water Conditions

Liangpeng Jiang,[a] Chunxia He,[a,*] Xiaolin Li,[a] and Jingjing Fu [b]

Wood–plastic composites (WPCs) are experiencing rapid growth in terms of applications where they may be subject to degradation and wear. This paper investigated the effect of sorghum straw (SS) fiber, pretreated with a mixture of stearic and palmitic acids, on the wear behaviors of polyvinyl chloride (PVC) composites in alternated simulated sea water and acid rain aqueous conditions. The results showed that the water resistance of the SS/PVC composites improved noticeably after pretreatment with 0.80 wt% stearic and 0.50 wt% palmitic acid (0.8SA-0.5PA). The SS/PVC composites pretreated with 0.8SA-0.5PA exhibited high water (moisture) resistance, hardness, mechanical, thermal, and wear resistance properties. Exposure to degradative water worsened interfacial bonding, and degraded the matrix strength and heat resistance, which reduced the wear resistance of the SS/PVC composites. The wear mechanism of the SS/PVC composites after 12 d of soaking was abrasive wear.

Keywords: Wood-plastic composites; Stearic acid; Palmitic acid; Degradation; Wear

*Contact information: a: College of Engineering, Nanjing Agricultural University, Nanjing 210031, China; b: Nanjing Research Institute for Agricultural Mechanization, Ministry of Agriculture, Nanjing 210014, China; *Corresponding author: chunxiahe@hotmail.com*

INTRODUCTION

Wood-plastic composites (WPCs) have emerged as potential eco-friendly and cost-effective alternatives to inorganic fiber polymeric composites. In the last decade, several major industries, such as the construction and building industries, have shown considerable interest in the progress of high-wear-resistance WPC materials (Omrani *et al.* 2016). Tribological analyses of WPCs such as jute/polypropylene, cotton/polyester, sisal/phenolic resin (or polyester), oil palm/polyester, sugarcane/polyester, kenaf/epoxy, betelnut/ polyester, and bamboo/epoxy have been performed (Chand and Dwivedi 2006, 2008; Hashmi *et al.* 2007; Xin *et al.* 2007; El-Tayeb 2008; Yousif and El-Tayeb 2008; Chin and Yousif 2009; Singh Gill *et al.* 2009; Nirmal *et al.* 2010, 2012).

It is known that WPCs would experience physical and mechanical degradation upon their exposure to external environmental conditions (such as temperature, humidity, and lighting). Therefore, there is a necessity for further study on the wear properties of WPCs in different aqueous environments (such as sea water and acid rain) to improve their durability (Nirmal *et al.* 2015). Yousif and Nirmal (2011) investigated the wear behavior of treated oil palm fiber-reinforced polyester (T-OPRP) composites exposed to different types of aging solutions (*i.e.*, distilled water, salt water, diesel, petrol, and engine oil). The researchers found that T-OPRP composites aged in distilled water and salt water exhibited poor wear resistance, while increasing trends in wear resistance were observed when the T-OPRP composites were aged in diesel, petrol, and engine oil. They claimed that diesel,

petrol, and engine oil were trapped in the surface pores of treated fiber during the aging process and acted as "lubricants" at the friction interfaces during the dry wear test.

One important method for enhancing the aging resistance of WPCs before exposure to high-moisture conditions is the formation of aquicludes within the fiber by pretreatment with a water-repellent admixture. Based on preliminary experiment data, the authors found that using the combination of stearic and palmitic acids in WPCs would obtain a better water resistance than using single acid. Hence, the current work aimed to explore the possibility of using a mixture of stearic and palmitic acids in sorghum straw fiber–reinforced polyvinyl chloride composites as a "degradation inhibitor" for alternated simulated sea water and acid rain degradative conditions.

EXPERIMENTAL

Materials

Sorghum straw (SS) was collected from local farmland in Nanjing, China. For fiber preparation, the air-dried SS was crushed to a particle size of 149 μm. Modification of the fiber was performed as follows: dipped in 4.5% sodium hydroxide (NaOH) at 100 °C for 1 h, rinsed with deionized water until neutral, and oven-dried at 90 °C for 24 h afterwards to eliminate residual humidity.

SG-5 polyvinyl chloride (PVC) was purchased from Tianye (Group) Co., Ltd., Xinjiang, China. Silane coupling agent KH-550 ($NH_2(CH_2)_3Si(OC_2H_5)_3$) was purchased from Chuangshi Chemical Additives Co., Ltd., Nanjing, China. The 603 non-toxic Ca/Zn composite stabilizer and H-108 polyethylene (PE) wax were purchased from Wenhua Chemical Pigment Co., Ltd., Shanghai, China. The stearic acid was purchased from Zhiyuan Chemical Reagent Co., Ltd., Tianjin, China. The palmitic acid was purchased from Sinopharm Chemical Reagent Co., Ltd., Beijing, China.

Sample preparation

The KH-550 (3 wt% with respect to the fiber) and absolute ethanol (volume ratio = 1:5) were mixed by manual agitation. The intermixture was sprayed evenly on the fibers. The fibers were dried at ambient temperature for 12 h followed by oven-drying at 90 °C for 12 h.

Silane-treated fiber, PVC, stabilizer, PE wax (mass ratio = 100:100:8:5), and different mass fractions of stearic and palmitic acid mixture were mixed by 3-D motion, and then extrusion-molded in a RM200C co-rotating twin-screw extruder (Hapro Electric Technology Co., Ltd., Harbin, China). The conical screw contained 4 temperature zones, and the processing temperatures varied in the range 150 °C to 165 °C. The screw rotational speed was 20 rpm, and the extruded profile had a cross-section of 7 mm × 10 mm.

Experimental design- Response surface design

To optimize the water resistances of SS/PVC composites, two different types of water-repellents (*i.e.*, stearic and palmitic acid) were blended for this study using response surface methodology (Stat-Ease/Design-Expert, version 8.0.6.1, Minneapolis, MN, USA). The response surface design used was defined by central composite design (CCD), and the response values were analyzed using the least squares method to fit the data (Eq. 1),

$$y = \beta_0 + \sum_{i=1}^{n} \beta_i x_i + \sum_{i=1}^{n} \beta_{ii} x_i^2 + \sum_{i=1}^{n-1} \sum_{j=i+1}^{n} \beta_{ij} x_i x_j + \varepsilon \quad (1)$$

where y is the predicted response, β_0, β_i, β_{ii}, and β_{ij} are the intercept, linear, quadratic and interaction terms, respectively, and x_i and x_j are the independent variables and ε is the residual term.

Three levels of stearic acid (or palmitic acid) content (with respect to the fibers) were chosen, as presented in Table 1. The response variable measured by experimentation was 24 h water absorption; details are provided in the physical and mechanical properties of the SS/PVC composites.

Table 1. Factors and Levels of Response Surface Design

Factor	Low Level (-1)	Medium Level (0)	High Level (+1)
Stearic acid (X_1, wt%)	0.5	1.5	2.5
Palmitic acid (X_2, wt%)	0.5	1.5	2.5

Degradation experimental design

In the authors' previous work it was found that exposure to aqueous conditions (such as deionized water, sea water, and acid rain) can significantly reduce the wear resistance of SS/PVC composites, and the worst exposure parameters were as follows: (a) first immersing in the simulated sea water at 55 ± 1 °C for 2 d and (b) then immersing in the simulated acid rain at 55 ±1 °C for 2 d, known simply as SW-AR-55&2 (Jiang *et al.* 2017a,b). In the present study, the worst exposure parameters were used to create a worst-case degradation scenario such as when WPC decking is installed in an acid rain region near the sea in the hot summer. Material behavior characterization (especially the wear resistance) was performed with the worst exposure parameters applied on the composites three times (*i.e.*, 12 d). For simulated sea water preparation, deionized water was adjusted to salinity 3.5% with sodium chloride (NaCl; CP, wt% ≥ 99.5). For simulated acid rain preparation, a sulfuric acid (H_2SO_4; purity 98%) and nitric acid (HNO_3; purity 68%) intermixture (with SO_4^{2-}:NO_3^- mole ratio = 5:1) was added to deionized water and kept at pH 2.5 (Jiang *et al.* 2017b).

Methods

Physical and mechanical properties of the SS/PVC composites

The physical properties were determined from 24 h water absorption (WA), 48 h moisture absorption (MA), and hardness tests according to the Chinese standards GB/T 17657 (2013), GB/T 20312 (2006), and GB/T 3398.1 (2008), respectively. An HH-600 thermostatic water tank (Baidian Instrument Equipment Co., Ltd., Shanghai, China) filled with deionized water and set at 23 °C ± 1 °C was used for WA testing. An HPX-160BSH-III temperature humidity incubator (CIMO Medical Instrument Manufacturing Co., Ltd., Shanghai, China) operating at 90% relative humidity and a temperature of 23 °C ± 0.5 °C was used for MA testing. The WA and MA values were calculated based on percentage weight gains. Prior to testing, the samples were dried at 90 °C for 12 h and weighed. After testing, the samples were re-weighed following the removal of surface water. An XHR-150 Plastics Rockwell hardness tester (Lianer Testing Equipment Co., Ltd., Shanghai, China) with indenter diameter of 12.7 mm and load of 60 kg (loading, unloading, and application times were 15 s, 15 s, and 5 s, respectively) was used for hardness testing.

The mechanical properties were determined from compressive, tensile, and flexural tests according to the Chinese standards GB/T 1041 (1992), GB/T 1040.1 (2006), and GB/T 9341 (2008), respectively. A CMT6104 electronic universal testing machine (MTS Industrial Systems Co., Ltd., Shanghai, China) with a loading speed of 2 mm·min^{-1} was used for testing.

Five replicate samples of each material at ambient temperature (25 °C ± 1 °C) were used for all physical and mechanical tests.

Fourier-transform infrared, thermogravimetric, and morphological analyses of the SS/PVC composites

Fourier-transform infrared (FTIR) spectra were recorded on a Nicolet iS10 FTIR spectrometer (Thermo Fisher Scientific Co., Ltd., Shanghai, China) in the range 400 cm^{-1} to 4000 cm^{-1} with resolution of 4 cm^{-1}.

Thermogravimetric (TG) tests were recorded on a STA 449 F3 synchronized thermal analyzer (NETZSCH Scientific Instrument Trading Co., Ltd., Selb, Germany) at a heating rate of 20 °C·min^{-1} under an argon atmosphere. The temperature ranged from 30 °C to 800 °C. The shielding and sweep gas rates were 20 mL·min^{-1} and 60 mL·min^{-1}, respectively.

Scanning electron microscopy (SEM) images were recorded using an S-4800 scanning electron microscope (Hitachi Ltd., Tokyo, Japan) with an acceleration voltage of 3 kV. Analytical surfaces were coated with gold layers using an E-1010 ion sputter coater (Hitachi Ltd., Tokyo, Japan).

Sliding wear tests of the SS/PVC composites

Dry sliding wear tests were conducted on an M-2000A Block On Ring Tribo machine (Xuanhua Kehua Testing Machine Manufacturing Co., Ltd., Zhangjiakou, China) at ambient temperature (25 °C ± 1 °C). The rotating ring, with outer diameter of 40 mm and surface hardness 40 HRC to 45 HRC, was made of quench-hardened 45# steel with surface roughness (R_a) 0.08 μm to 0.12 μm. The block sample (6 × 7 × 30 mm^3) was subjected to a fixed normal load (100 N), constant sliding velocity (200 rpm), and different sliding times (30 min, 60 min, 90 min, and 120 min). Prior to each test, the sample and counterface were cleaned with absolute ethanol and air-dried. Three replicate samples of each material were used to assess wear resistance.

The average friction coefficient (μ) was directly obtained from the device *via* a transducer attached to the tribo machine and recorded by computer interface. The volumetric wear (ΔV, mm^3) was calculated from the weight loss and the density of the sliding sample. Weight loss was measured using a FA1004 electronic analytical balance (0.1 mg sensitivity) (Hengping Scientific Instrument Co., Ltd., Shanghai, China), and density was measured using a DH-300 direct-reading electronic densimeter (Dahometer Instrument Co., Ltd., Dongguan, China). The specific wear rate (W_S) was calculated using Eq. 1 (Jeamtrakull *et al.* 2012), where F is the normal load (N) and L is the sliding distance (m):

$$W_S = \frac{\Delta V}{F \cdot L} \quad (1)$$

RESULTS AND DISCUSSION

Analysis of Response Surface Experiment

Analysis of variance

Table 2 presents the response surface design and results for the 24 h water absorption of the SS/PVC composites; the variance analysis is presented in Table 3. In summary, 13 experiments were statistically analyzed to assess the significance of the factor variables. The determination coefficient (R^2) value was 95.02%; the closeness of this value to one indicated a high degree of correlation between the observed and predicted values. Only 4.98% of the total variation was not explained by the present model. According to Owolabi *et al.* (2018), adjusted determination coefficient (R_{adj}^2) and predicted determination coefficient (R_{pred}^2) should be within 20% to be in good agreement. This requirement is satisfied in this study with a R_{adj}^2 value of 91.45% and R_{pred}^2 value of 78.03%. The P-values were less than 0.05 (except for X_1X_2) with high F-values (except for X_1X_2), which indicated that all factor variables were statistically significant in the optimization. The lack-of-fit (P-value) was 0.36 (> 0.05), which indicated the adequacy of the model to accurately predict variation.

Table 2. Response Surface Design and Results for the 24 h Water Absorption of the SS/PVC Composites

Sample ID	X_1 (wt%)	X_2 (wt%)	24 h WA (%)
L_1	0.50	0.50	0.99 ± 0.04
L_2	2.50	0.50	1.27 ± 0.05
L_3	0.50	2.50	1.25 ± 0.13
L_4	2.50	2.50	1.50 ± 0.11
L_5	0.09	1.50	1.10 ± 0.04
L_6	2.91	1.50	1.39 ± 0.06
L_7	1.50	0.09	1.05 ± 0.05
L_8	1.50	2.91	1.30 ± 0.07
L_9	1.50	1.50	1.14 ± 0.03
L_{10}	1.50	1.50	1.07 ± 0.01
L_{11}	1.50	1.50	1.08 ± 0.07
L_{12}	1.50	1.50	1.12 ± 0.08
L_{13}	1.50	1.50	1.03 ± 0.02

Table 3. Variance Analysis of Response Surface Design and Results

Source	Sum of Squares	DF	Mean Square	F-value	P-value
Model	0.27	5	0.05	26.69	< 0.01
X_1	0.11	1	0.11	55.81	< 0.01
X_2	0.09	1	0.09	43.34	< 0.01
X_1X_2	3.19E-004	1	3.19 E-004	0.16	0.70
X_1^2	0.06	1	0.06	28.32	< 0.01
X_2^2	0.02	1	0.02	9.49	0.02
Residual	0.01	7	2.01E-003		
Lack of fit	7.22E-003	3	2.41E-003	1.40	0.36
Pure error	6.86E-003	4	1.71E-003		
Total	0.28	12			
R^2 = 95.02%, R_{adj}^2 = 91.45%, and R_{pred}^2 = 78.03%					

Optimization of water resistance

The 3-D response surface and 2-D counter plots were utilized to visualize the effects of the factor variables on the response variables, as shown in Fig. 1. In the experimental range, the 24 h WA values decreased overall with the decrease of each factor variable, then slightly increased after reaching a minimum. From the 2-D contour plots, strong interaction effects existed between two factor variables with regard to the 24 h WA values when their values were low, because the curvatures of isolines in those regions were high.

The minimum 24 h WA value (0.99%) was found when stearic and palmitic acid contents were 0.80 wt% and 0.50 wt%, respectively. A practical experiment was conducted to verify the prediction. The actual 24 h WA value was 1.02% ± 0.02%, which was extremely close to the predicted value of 0.99%. This further confirmed the validity of the optimal conditions.

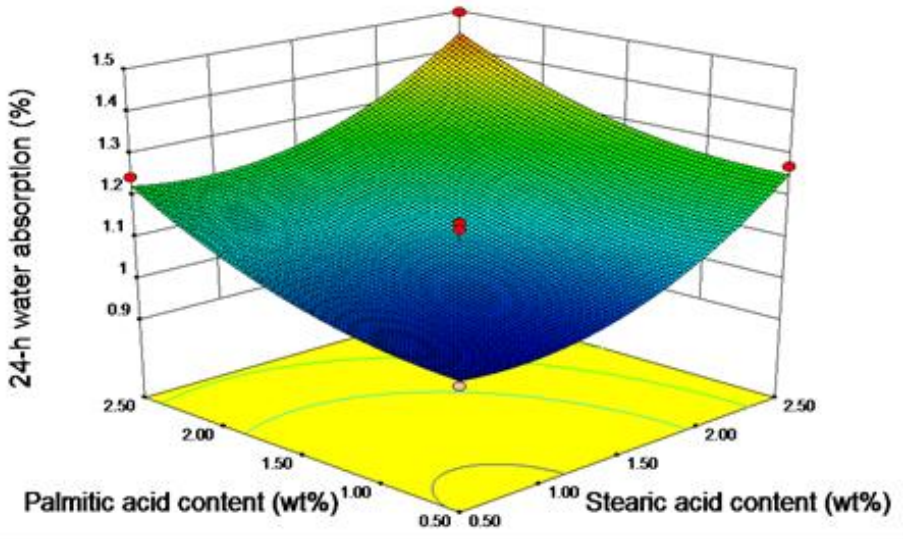

Fig. 1. 3-D response surface and 2-D counter plots for the effects of the factor variables on the response variables

Water and Moisture Absorption Analyses of the SS/PVC Composites

The 24 h water and 48 h moisture absorptions of the SS/PVC composites are presented in Fig. 2. The optimized SS/PVC composites (OSPCs) had noticeably lower water (or moisture) absorption than the un-optimized SS/PVC composites (USPCs), except that samples with a long period of exposure exhibited a slight increase in water (or moisture) absorption. Water (or moisture) within WPC materials can exist in two regions: fiber cells (wall and lumen) and gaps between fiber and matrix (Hosseinaei *et al.* 2012). Based on this theory, it can be inferred that stearic acid (0.80 wt%) and palmitic acid (0.50 wt%) as a mixture (0.8SA-0.5PA) will reduce interfacial gaps and limit the penetration of water (or moisture) into these gaps. However, although 0.8SA-0.5PA effectively eliminated penetration of water (or moisture) into SS/PVC composites, long-time absorption of degradative water (*i.e.*, sea water and acid rain) will still attack the two-phase interface, resulting in degradation of interfacial integrity and increased water (or moisture) absorption.

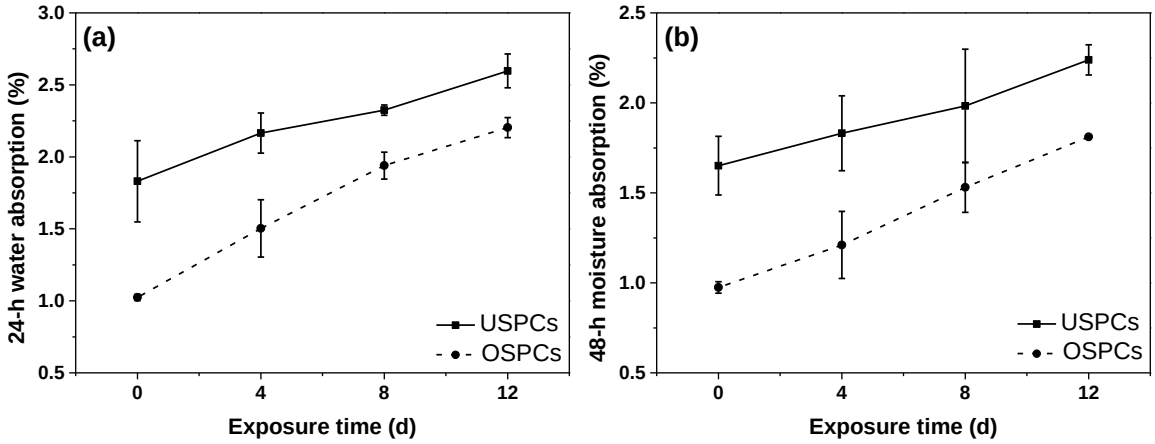

Fig. 2. 24 h water and 48 h moisture absorption of the SS/PVC composites

Physical and Mechanical Properties of the SS/PVC Composites

The physical and mechanical properties of the SS/PVC composites are presented in Fig. 3. The OSPCs had higher physical (*i.e.*, hardness) and mechanical (*i.e.*, compressive, tensile, and flexural strength) properties than the USPCs for different exposure durations, presumably due to better interaction (*i.e.*, mechanical interlock) between the fiber and matrix in the presence of 0.8SA-0.5PA.

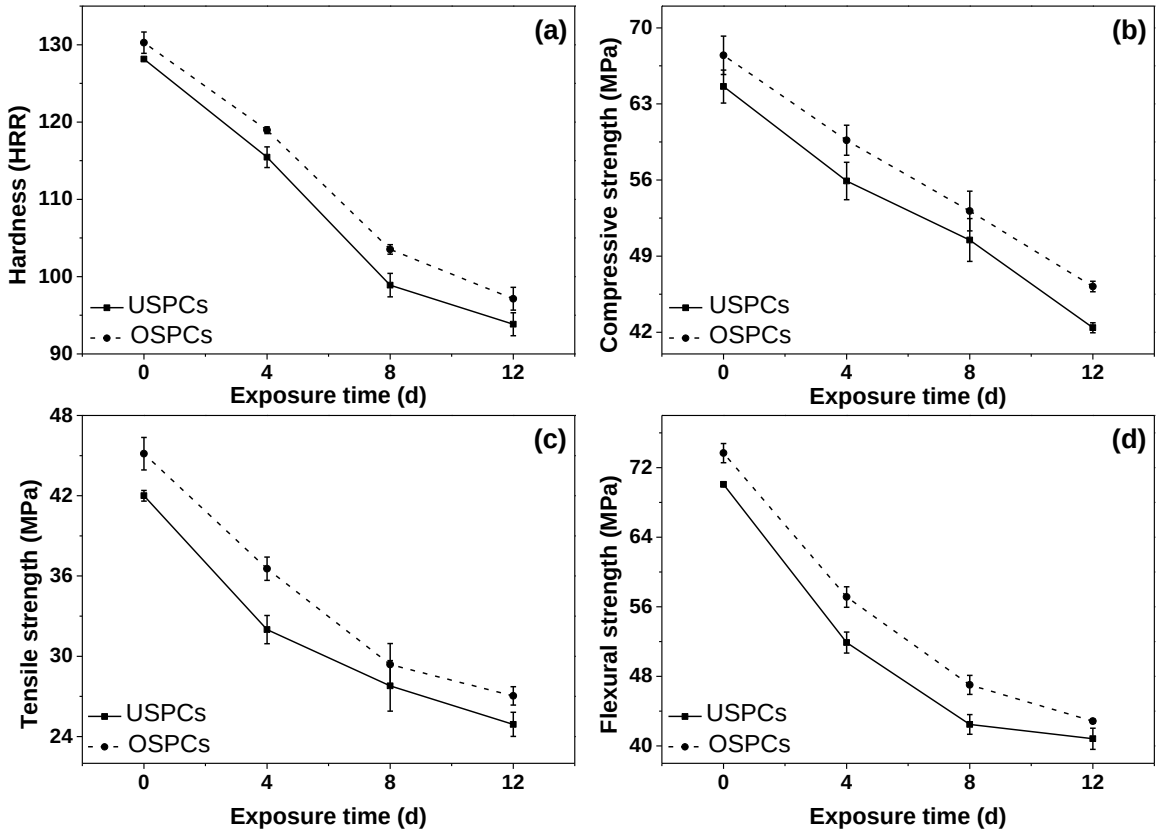

Fig. 3. Physical and mechanical properties of the SS/PVC composites

Alternate degradation conditions reduced the physical and mechanical properties of both USPCs and OSPCs. Specifically, the reductions of hardness and compressive, tensile, and flexural strengths after exposure to SW-AR-55&2 for 3 times (*i.e.*, 12 d) were 26.77%, 34.35%, 40.69%, and 41.74%, respectively, for USPCs, and 25.43%, 31.52%, 40.10%, and 41.85%, respectively, for OSPCs. Decreases in the physical and mechanical properties were probably due to the absorption of degradative water. Degradative water attacks fiber which caused the damage of the structure and properties of fiber (Dhakal *et al.* 2007). Water-swelling of fiber can also form shear stresses between two-phase interfaces. Those result in the deterioration of compatibility between fiber and matrix, and facilitate the de-bonding of fiber from the matrix.

Fracture Surfaces Analysis of the SS/PVC Composites

Figures 4(a) and 4(b) present the tensile fracture surfaces of the non-degraded USPCs and OSPCs, respectively. Fibers were enveloped by matrix and pull-out fibers, and de-bonding in the two-phase interface was not observed (interfacial quality: Fig. (b) > Fig. (a)). In the tensile fracture surfaces of USPCs and OSPCs after exposure to SW-AR-55&2 for 3 times (*i.e.*, 12 d) (Figs. 4(c) and (d)), pulled-out fibers and de-bonding in the two-phase interface were observed, which suggested poor interfacial bonding between the fiber and matrix (interfacial quality: Fig. (d) > Fig. (c)). Gaps created in the two-phase interface facilitated the penetration of water (or moisture) into the samples, which was evidence of water and moisture absorption analyses of the SS/PVC composites, and negatively affected the transfer of stress from matrix to fibers.

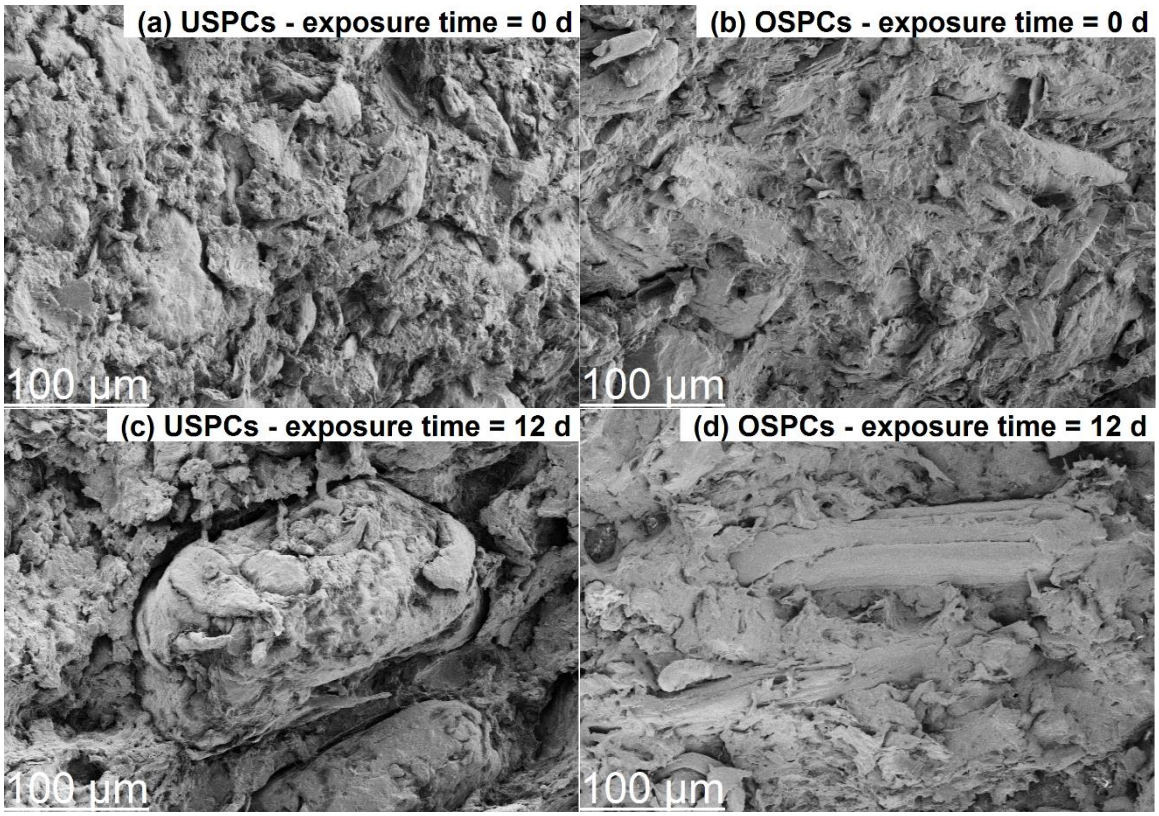

Fig. 4. SEM micrographs of the tensile fracture surfaces of the SS/PVC composites

Friction and Wear Properties of the SS/PVC Composites

Friction coefficients and specific wear rates of the SS/PVC composites are presented in Fig. 5. The μ and W_S values of the OSPCs were noticeably smaller than the USPCs at the same sliding time under different exposure durations. This was explained by 0.8SA-0.5PA filling micro-gaps between the fiber and matrix, which resulted in enhanced interfacial bonding.

In general, the wear resistance of both USPCs and OSPCs decreased with an increased exposure period. This was because better interfacial bonding in samples prevented de-bonding of the fiber from the matrix and improved matrix strength. A decrease in de-bonding probability of fiber can effectively avoid the formation of abrasive particles. An increase in matrix strength can also reduce the real contact and frictional force of the sliding interface. However, the quality of interfacial bonding reduced with increased exposure period, as mentioned earlier.

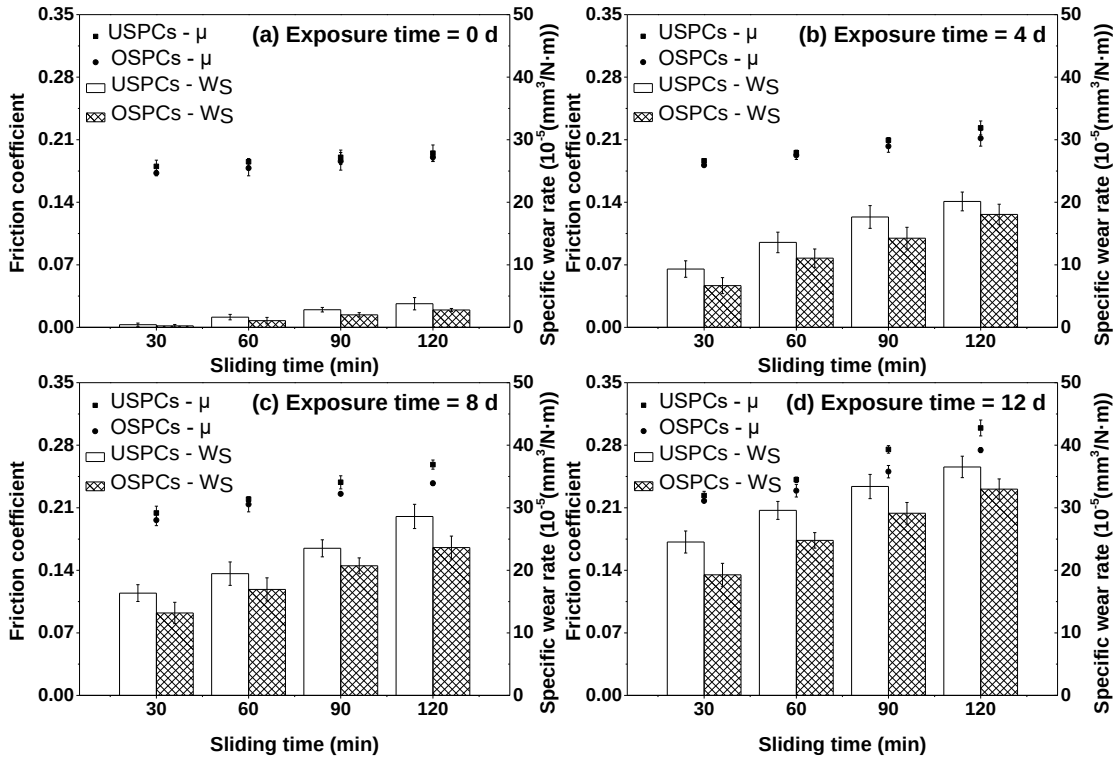

Fig. 5. Friction coefficients and specific wear rates of the SS/PVC composites

FTIR Analysis of the SS/PVC Composites

The FTIR and TG analyses of the tested materials were performed to comprehensively identify the causes of difference in wear behavior at the chemical and thermal levels.

The FTIR spectra of the SS/PVC composites are presented in Fig. 6. The typical vibration bands of SS/PVC composites included 3500 cm^{-1} to 3300 cm^{-1} (O–H stretching, fiber), 2935 cm^{-1} to 2900 cm^{-1} (C–H asymmetrical stretching, fiber, and PVC), 1735 cm^{-1} to 1700 cm^{-1} (C=O stretching, fiber), 1515 cm^{-1} to 1505 cm^{-1} (aromatic skeleton vibrations), 1425 cm^{-1} (C–H deformation, fiber, and PVC), 1250 cm^{-1} to 1230 cm^{-1} (C–O and Si–C stretching, fiber), 1100 cm^{-1} to 970 cm^{-1} (C–O stretching and C–C deformation,

fiber, and PVC), and 700 cm^{-1} to 600 cm^{-1} (C–Cl stretching, PVC) (Islam *et al.* 2012; Migneault *et al.* 2015; Zierdt *et al.* 2015; Machado *et al.* 2016). The vibration band at the range of 3500 to 3300 cm^{-1} became weaker with the addition of 0.8SA-0.5PA and the increasing exposure duration, which indicated that encapsulation of the fiber formed by 0.8SA-0.5PA. And the simulated sea water and acid rain immersion possessed similar effect as fiber pretreatment (such as alkali treatment, acid treatment, and hydrothermal treatment). It should be noted that all of the samples had similar chemical structures (*i.e.*, functional groups), which indicated that the differences in wear behavior of SS/PVC composites were not due to the differences in chemical structure among the materials tested.

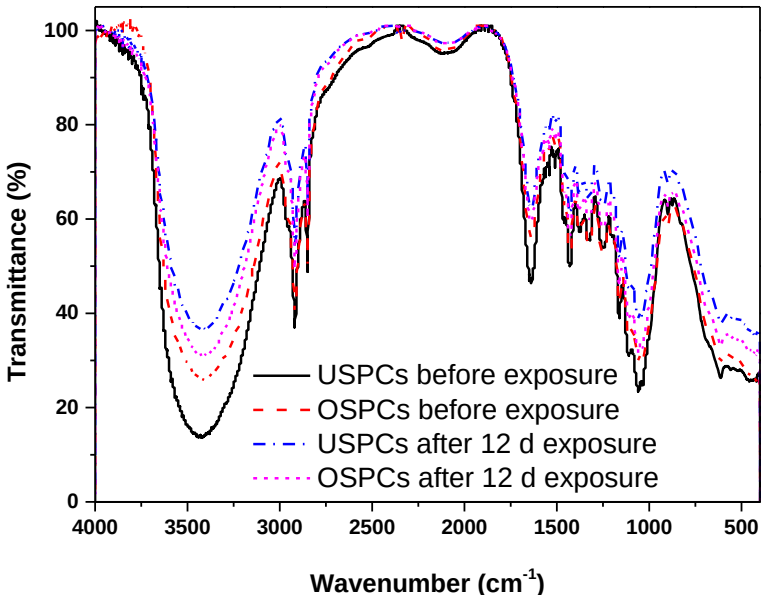

Fig. 6. FTIR spectra of the SS/PVC composites

Thermogravimetric Analysis of the SS/PVC Composites

The TG curves of the PVC and SS/PVC composites are presented in Fig. 7. Thermal degradation of the SS/PVC composites occurred over a wide temperature range (260 °C to 500 °C). The four TG curves were divided into two stages of weight loss: before 150 °C, when volatilization of free and bound water occurred, and after 150 °C, when the degradation of hemicellulose, cellulose, and lignin (main components of the lignocellulosic materials) occurred in the temperature ranges of 200 °C to 350 °C, 275 °C to 350 °C, and 250 °C to 500 °C, respectively (Jeske *et al.* 2012; Barton-Pudlik *et al.* 2017). In addition, PVC degradation mainly occurred in the temperature range of 285.6 °C to 352.3 °C, forming de-HCl PVC and volatiles, such as HCl, benzene, toluene, and other hydrocarbons, and cracking and decomposition of the de-HCl PVC occurred in the temperature range of 439.9 °C to 485.2 °C. Based on the TG curves, it is concluded that the SS/PVC composites showed lower thermal stabilities in comparison with pure PVC.

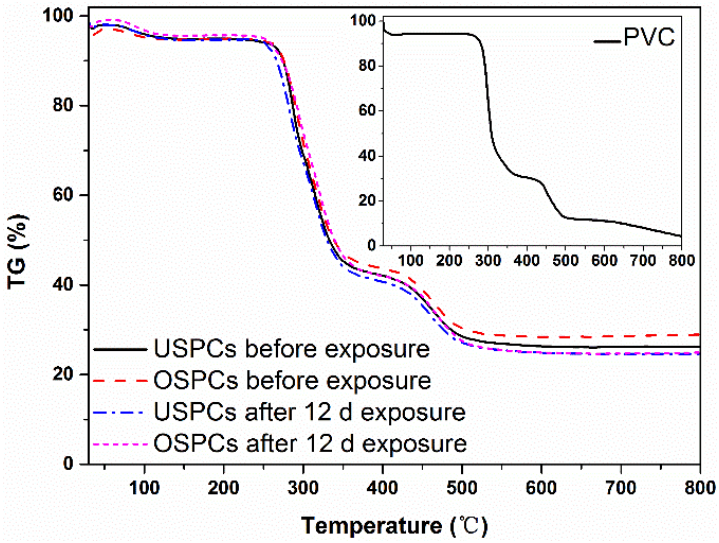

Fig. 7. TG curves of the PVC and SS/PVC composites

The TG properties of the PVC and SS/PVC composites are presented in Table 4, which was the basis for further assessing the thermal behaviors of USPCs and OSPCs. The addition of 0.8SA-0.5PA slightly increased the thermal stabilities of SS/PVC composites, although the trend was not obvious. This enhanced heat resistance indicated the improved wear resistance, because a high heat resistance limited the thermal softening of the polymer matrix in the friction heat-accumulation environment, inhibiting the production of adhesive contacts. However, the degradation temperature and mass loss shifted to lower values with increasing exposure duration. This behavior was attributed to the deterioration effect of degradative water absorption on the bonding strength between two phases, which decreased the deformation resistance of the polymer molecular chain, resulting in low thermal stability.

Table 4. TG Properties of the PVC and SS/PVC Composites

Sample ID	Exposure Time (d)	Pyrolysis process					
		First Stage			Second Stage		
		Temperature (°C)		Mass Loss (%)	Temperature (°C)		Mass Loss (%)
		Onset	Termination		Onset	Termination	
PVC	~	285.6	352.3	64.1	439.9	485.2	21.2
USPCs	0	273.7	342.7	53.5	439.5	491.3	16.6
	12	263.2	337.2	50.7	435.6	485.5	16.5
OSPCs	0	273.8	343.7	54.0	442.0	492.8	16.9
	12	267.1	337.2	52.2	435.3	488.6	16.5

Wear Mechanisms of the SS/PVC Composites

The SEM micrographs of the worn surfaces of the SS/PVC composites are presented in Fig. 8. As shown in Fig. 8(a), numerous scratches and grooves were distributed on the worn surface of USPCs. Scratches and grooves are the characteristics of abrasive wear that resulted from cutting and plowing of micro-bulges on the counterface (*i.e.*, hard abrasive wear), or from linked fiber debris detached by the counterface (*i.e.*, soft abrasive wear). In the soft abrasive wear process, high-speed soft fibers resulted from repeated action (such as extruding and rubbing) of the normal and tangential forces in high-

temperature and high-loading environments. As a result, molecules reunite and bond mutually to form "incompressible lumps", *i.e.*, another form of hard particle (Zhang *et al.* 2016a,b, 2017). Melting wear should be considered when analyzing the wear mechanism in thermoplastic polymeric composites because the melting temperature and thermal conductivity of thermoplastic polymers (including PVC) are generally low, which could increase the frictional interface temperature to the melting temperature of the polymer matrix.

In Fig. 8(b), scratches and grooves were shallower and smoother than those in Fig. 8(a). The results of the comparison further demonstrated that pretreatment with 0.8SA-0.5PA improved the wear resistances of SS/PVC composites.

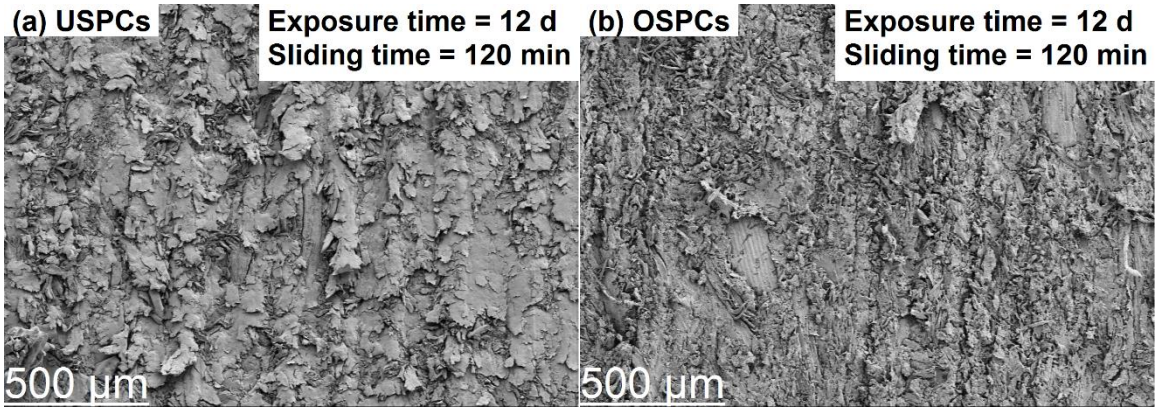

Fig. 8. SEM micrographs of the worn surfaces of the SS/PVC composites

CONCLUSIONS

1. Under the experimental conditions, SS fiber pretreated with 0.8SA-0.5PA endowed SS/PVC composites with high water resistance (an indirect reflection of high quality of interfacial bonding) relative to other ratios of stearic and palmitic acid.
2. In comparison to the USPCs, the OSPCs exhibited lower 24-h water absorption (down 44.07%) and 48-h moisture absorption (down 40.95%), and higher hardness (up 1.65%), compressive strength (up 4.45%), tensile strength (up 7.48%), flexural strength (up 5.13%), as well as better heat and wear resistance before immersion in degradative water conditions (successive soaking in simulated sea water, followed by simulated acid rain). In addition, the OSPCs also exhibited better performance than those of USPCs under any condition in this work.
3. The interfacial bonding quality of the SS/PVC composites decreased after their immersion in degradative water conditions, which reduced the matrix strength and heat resistance, and thus increased the adhesive contact and the frictional force. High-speed soft fiber debris formed in high-temperature and high-loading frictional environments can be deemed a type of "hard particle" that form hard abrasive wear.

ACKNOWLEDGEMENTS

This work was supported by the National Science and Technology Support Program (China), Grant No. 2011BAD20B202-2.

REFERENCES CITED

Barton-Pudlik, J., Czaja, K., Grzymek, M., and Lipok, J. (2017). "Evaluation of wood-polyethylene composites biodegradability caused by filamentous fungi," *International Biodeterioration & Biodegradation* 118, 10-18. DOI: 10.1016/j.ibiod.2017.01.014

Chand, N., and Dwivedi, U. K. (2006). "Effect of coupling agent on abrasive wear behaviour of chopped jute fibre-reinforced polypropylene composites," *Wear* 261(10), 1057-1063. DOI: 10.1016/j.wear.2006.01.039

Chand, N., and Dwivedi, U. K. (2008). "Sliding wear and friction characteristics of sisal fibre reinforced polyester composites: Effect of silane coupling agent and applied load," *Polymer Composites* 29(3), 280-284. DOI: 10.1002/pc.20368

Chin, C. W., and Yousif, B. F. (2009). "Potential of kenaf fibres as reinforcement for tribological applications," *Wear* 267(9-10), 1550-1557. DOI: 10.1016/j.wear.2009.06.002

Dhakal, H. N., Zhang, Z. Y., and Richardson, M. O. W. (2007). "Effect of water absorption on the mechanical properties of hemp fibre reinforced unsaturated polyester composites," *Composites Science and Technology* 67(7-8), 1674-1683. DOI: 10.1016/j.compscitech.2006.06.019

El-Tayeb, N. S. M. (2008). "A study on the potential of sugarcane fibers/polyester composite for tribological applications," *Wear* 265(1-2), 223-235. DOI: 10.1016/j.wear.2007.10.006

GB/T 1040.1 (2006). "Plastic - Determination of tensile properties," Standardization Administration of China, Beijing, China.

GB/T 1041 (1992). "Plastic - Determination of compressive properties," Standardization Administration of China, Beijing, China.

GB/T 3398.1 (2008). "Plastic - Determination of hardness," Standardization Administration of China, Beijing, China.

GB/T 9341 (2008). "Plastic - Determination of flexural properties," Standardization Administration of China, Beijing, China.

GB/T 17657 (2013). "Test methods of evaluating the properties of wood–based panels and surface decorated wood–based panels," Standardization Administration of China, Beijing, China.

GB/T 20312 (2006). "Hygrothermal performance of building materials and products - Determination of hygroscopic sorption properties," Standardization Administration of China, Beijing, China.

Hashmi, S. A. R., Dwivedi, U. K., and Chand, N. (2007). "Graphite modified cotton fibre reinforced polyester composites under sliding wear conditions," *Wear* 262(11-12), 1426-1432. DOI: 10.1016/j.wear.2007.01.014

Hosseinaei, O., Wang, S., Taylor, A. M., and Kim, J. W. (2012). "Effect of hemicellulose extraction on water absorption and mold susceptibility of wood–plastic composites," *International Biodeterioration & Biodegradation* 71, 29-35. DOI: 10.1016/j.ibiod.2011.12.015

Islam, M. S., Hamdan, S., Hasan, M., Ahmed, A. S., and Rahman, M. R. (2012). "Effect of coupling reactions on the mechanical and biological properties of tropical wood polymer composites (WPC)," *International Biodeterioration & Biodegradation* 72, 108-113. DOI: 10.1016/j.ibiod.2012.05.019

Jeamtrakull, S., Kositchaiyong, A., Markpin, T., Rosarpitak, V., and Sombatsompop, N. (2012). "Effects of wood constituents and content, and glass fiber reinforcement on wear behavior of wood/PVC composites," *Composites Part B: Engineering* 43(7), 2721-2729. DOI: 10.1016/j.compositesb.2012.04.031

Jeske, H., Schirp, A., and Cornelius, F. (2012). "Development of a thermogravimetric analysis (TGA) method for quantitative analysis of wood flour and polypropylene in wood plastic composites (WPC)," *Thermochimica Acta* 543, 165-171. DOI: 10.1016/j.tca.2012.05.016

Jiang, L. P., He, C. X., Fu, J. J., and Chen, D. M. (2017a). "Wear behavior of wood-plastic composites in alternate simulated sea water and acid rain corrosion conditions," *Polymer Testing* 63, 236-243. DOI: 10.1016/j.polymertesting.2017.08.031

Jiang, L. P., He, C. X., Fu, J. J., and Chen, D. M. (2017b). "Wear behavior of straw fiber-reinforced polyvinyl chloride composites under simulated acid rain conditions," *Polymer Testing* 62, 373-381. DOI: 10.1016/j.polymertesting.2017.07.028

Machado, J. S., Santos, S., Pinho, F. F. S., Luís, F., Alves, A., Simões, R., and Rodrigues, J. C. (2016). "Impact of high moisture conditions on the serviceability performance of wood plastic composite decks," *Materials & Design* 103, 122-131. DOI: 10.1016/j.matdes.2016.04.030

Migneault, S., Koubaa, A., Perré, P., and Riedl, B. (2015). "Effects of wood fiber surface chemistry on strength of wood-plastic composites," *Applied Surface Science* 343, 11-18. DOI: 10.1016/j.apsusc.2015.03.010

Nirmal, U., Yousif, B. F., Rilling, D., and Brevern, P. V. (2010). "Effect of betelnut fibres treatment and contact conditions on adhesive wear and frictional performance of polyester composites," *Wear* 268(11-12), 1354-1370. DOI: 10.1016/j.wear.2010.02.004

Nirmal, U., Hashim, J., and Low, K. O. (2012). "Adhesive wear and frictional performance of bamboo fibres reinforced epoxy composite," *Tribology International* 47, 122-133. DOI: 10.1016/j.triboint.2011.10.012

Nirmal, U., Hashim, J., and Ahmad, M. M. H. M. (2015). "A review on tribological performance of natural fibre polymeric composites," *Tribology International* 83, 77-104. DOI: 10.1016/j.triboint.2014.11.003

Omrani, E., Menezes, P. L., and Rohatgi, P. K. (2016). "State of the art on tribological behavior of polymer matrix composites reinforced with natural fibers in the green materials world," *Engineering Science and Technology, an International Journal* 19(2), 717-736. DOI: 10.1016/j.jestch.2015.10.007

Owolabi, R. U., Usman, M. A., and Kehinde, A. J. (2018). "Modelling and optimization of process variables for the solution polymerization of styrene using response surface methodology," *Journal of King Saud University-Engineering Sciences* 30(1), (22-30). DOI: 10.1016/j.jksues.2015.12.005

Singh Gill, N., and Yousif, B. F. (2009). "Wear and frictional performance of betelnut fibre-reinforced polyester composite," *Proceedings of the Institution of Mechanical Engineers,* 10.1243/13506501JET516*Part J: Journal of Engineering Tribology* 223(2), 183-194. DOI:

Xin, X., Xu, C. G., and Qing, L. F. (2007). "Friction properties of sisal fibre reinforced resin brake composites," *Wear* 262(5-6), 736-741. DOI: 10.1016/j.wear.2006.08.010

Yousif, B. F., and El-Tayeb, N. S. M. (2008). "Adhesive wear performance of T-OPRP and UT-OPRP composites," *Tribology Letters* 32(3), 199-208. DOI: 10.1007/s11249-008-9381-7

Yousif, B. F., and Nirmal, U. (2011). "Wear and frictional performance of polymeric composites aged in various solutions," *Wear* 272(1), 97-104. DOI: 10.1016/j.wear.2011.07.006

Zhang, K. P., Jiang, L. P., and Huang, X. P. (2016a). "Heat treatment process optimization of roller material of wheat mill against abrasive wear," *Transactions of the Chinese Society of Agricultural Engineering* 32(21), 271-276. DOI: 10.11975/j.issn.1002-6819.2016.21.037.

Zhang, K. P., Jiang, L. P., and Wang, J. X. (2016b). "Wheat powder abrasion wear resistance of white cast iron with different chromium content," *Materials for Mechanical Engineering* 40(12), 57-60. DOI: 10.11973/jxgccl201612013

Zhang, K. P., Jiang, L. P., and Yao, Y. P. (2017). "Experiment of white iron abrasive wear for wheat grain powder," *Journal of the Chinese Cereals and Oils Association* 32(1), 109-112. DOI: 10.3969/j.issn.1003-0174.2017.01.019

Zierdt, P., Theumer, T., Kulkarni, G., Däumlich, V., Klehm, J., Hirsch, U., and Weber, A. (2015). "Sustainable wood-plastic composites from bio-based polyamide 11 and chemically modified beech fibers," *Sustainable Materials and Technologies* 6, 6-14. DOI: 10.1016/j.susmat.2015.10.001

Article submitted: January 14, 2018; Peer review completed: April 2, 2018; Revised version received: March 30, 2018; Further revised version accepted: April 2, 2018; Published: April 16, 2018.
DOI: 10.15376/biores.13.2.3817-3831